Sensorimotor cortex atrophy in patients with cervical spondylotic myelopathy

Lanbo Wang[a], Bing Yu[a], Qun Li[a], Fei Qi[b] and Qiyong Guo[a]

Previous studies have shown compensatory adaptive changes in cerebral functions before surgery in patients with cervical spondylotic myelopathy (CSM), especially in the sensorimotor cortices. However, the structural changes in the sensorimotor cortices in patients with CSM remain poorly understood. The aim of this study was to assess the volumetric changes in the sensorimotor cortices using morphological MRI and to correlate these changes with clinical scales. We hypothesize that CSM causes atrophy in the sensorimotor cortices, which results in functional changes during CSM progression. The study participants included 30 CSM patients and 25 matched healthy controls. The patients underwent brain morphological MRI before surgery. Compared with the healthy controls, the patients with CSM showed significant atrophy in the primary somatosensory cortex (S1), the primary motor cortex (M1), the somatosensory association cortex, and the supplementary motor area. The gray matter volumes in the S1 and M1 were correlated positively with the motor scores of the Japanese Orthopedic Association in patients with CSM. The change in supplementary motor area correlated with the sphincter scores of the Japanese Orthopedic Association in CSM patients. Our findings provide new insights into the compensatory reaction in CSM patients. *NeuroReport* **29:826–832**

NeuroReport 2018, **29**:826–832

Keywords: cervical spondylotic myelopathy, cortical reorganization, morphological magnetic resonance imaging, sensorimotor cortex

Departments of [a]Radiology and [b]Orthopedic Surgery, Shengjing Hospital of China Medical University, Shenyang, Liaoning, China

Correspondence to Qiyong Guo, MD, Department of Radiology, Shengjing Hospital of China Medical University, Shenyang, Liaoning 110004, China
Tel: +86 249 6615, fax: +86 242 392 9902; e-mail: guoqiyongcmu@163.com

Received 5 December 2017 **accepted** 2 April 2018

Introduction

Cervical spondylotic myelopathy (CSM), a common form of chronic myelopathy, is caused by the degeneration of an intervertebral disk, which results in limb dysfunction, sensory loss, and pain. The traditional therapy focuses on the spinal column and spinal cord abnormalities because CSM is associated with local compressive impairment. However, spinal cord compression affects the permanent cerebral structure, causing functional reorganization with a long-term loss of sensory input and motor output stimulatory. Increasing evidence indicates that motor efferents and sensory afferents are disrupted in animal models with spinal cord injury, leading to volumetric reductions in the sensorimotor cortex [1,2].

It has been noted that sensorimotor cortical atrophy occurs in the primary motor cortex (M1), the primary somatosensory cortex (S1), the supplementary motor area (SMA), and the thalamic area in patients with spinal cord injury (SCI) [3,4]. As a specific SCI, the CSM has similar local damage with SCI. Several studies have detected brain reorganization in patients with CSM. Furthermore, cerebral functional reorganization has been detected with task-state functional MRI (fMRI) [5–11]. More specifically, results of resting-state-fMRI research have shown enhanced activation in the sensorimotor cortices of CSM patients [8,9]. All the tasks that were tested showed that cortical reorganization occurs in CSM patients and coincides with structural changes. Therefore, CSM may lead to structural changes in the sensorimotor system.

The sensorimotor system includes the M1, S1, the somatosensory association cortex (SAC), and SMA. As such, the primary somatosensory cortex is equivalent to Brodmann area 1 (BA1), BA2, and BA3. BA3 can be subdivided into BA3a and BA3b [12], and M1 can be subdivided to the anterior (BA4a) and posterior parts (BA4p) [13,14]. All of the aforementioned subdivisions have distinct receptor density characteristics and cytoarchitecture, which reflect their different functions [15].

The mean age of CSM patients is 68.7 years and it predominantly affects men older than 70 years of age [16]. Consequently, brain degeneration may already be present in this patient population, which would influence the results of any volumetric imaging. Therefore, to alleviate this confounding variable, we focused on patients younger than 65 years of age.

On the basis of previous studies, we hypothesized (a) that patients with CSM would show gray matter atrophy in the subdivision structures of their sensorimotor cortices and (b) that the structural atrophy in these areas would correlate with the Japanese Orthopedic Association (JOA) scores of CSM patients. To test our hypotheses, we used voxel-based morphometry to investigate the structural changes in the gray matter of CSM patients.

Materials and methods

This is a cross-sectional prospective study. The study was approved by the Institutional Review Board of Shengjing

DOI: 10.1097/WNR.0000000000001039

Hospital, China Medical University, Shenyang, China. Before the study, all the participants provided their written informed consent, according to the principles of the Declaration of Helsinki.

Participants

A total of 55 right-handed participants (30 CSM patients and 25 healthy controls, mean age: 51.25 ± 7.55 years) were recruited during a 13-month period between July 2016 and August 2017. All the patients with CSM had clear evidence of cord compression on cervical spinal images, including ligamentum flavum hypertrophy, cervical spondylosis, and herniated discs. The exclusion criteria for the study were as follows: (a) younger than 30 years of age or older than 65 years of age; (b) no requirement for surgical treatment; (c) past or present history of a serious physical or neurological disease; (d) past or present history of depression, anxiety, substance abuse, or other mental illnesses; (e) history of mental or neurological disease in the immediate family; (f) brain abnormality (tumor, hemorrhage, or infarct) found with routine MRI; and (g) MRI contraindications.

Before scanning, the JOA questionnaire was completed by all the participants to measure their neurological functions. The first structural scan was performed the week before decompressive surgery. Clinical and demographic data for all the participants are shown in Table 1.

MRI data acquisition

Each participant was scanned using a 3.0-T MRI system scanner (Ingenia; Philips Medical Systems, Best, The Netherlands) with 15 Sensitivity Encoding (SENSE) head coils. A high-resolution 3D Turbo Field Echoing T1WI structural scan was performed with the following parameters: TR 7.25 ms; TE 3.44 ms; flip angle 8°; FOV 256 mm; matrix 256 × 256; layers 226; and section thickness 1.6 mm.

Structural data preprocessing

The voxel-based morphometry preprocessing and statistical analyses were carried out using the Statistical Parametric Mapping (SPM12) software (*http://www.fil.ion.ucl.ac.uk/spm/*), implemented in MATLAB 2012b (MathWorks, Natick, Massachusetts, USA). The MRI were first segmented into gray matter, white matter, and cerebrospinal fluid with the unified segmentation module [17]. These segmented gray and white matter images were used to obtain an accurate interpatient registration model using DARTEL [18]. This model alternates between computing a group template and warping an individual's tissue probability map into alignment with the template, which ultimately creates an individual flow field for each participant [19,20]. The images of each participant were normalized to Montreal Neurological Institute (MNI) space. The normalized images were modulated to ensure that the relative gray and white matter volumes were well preserved after spatial normalization. Finally, these images were smoothed with an 8 mm full-width at half-maximum Gaussian kernel.

Table 1 Demographic and clinical characteristics of cervical spondylotic myelopathy patients and controls

Characteristics	Patients	Healthy control	*P* value
n	30	25	N/A
Age	51.32 ± 7.52	51.2 ± 7.71	0.95
Sex (male/female)	19/11	11/14	N/A
Handedness (right/left)	30/0	25/0	N/A
JOA scores	10.80 ± 2.84	17 ± 0	< 0.0001
Motor upper	2.63 ± 1.13	4 ± 0	< 0.0001
Motor lower	2.73 ± 0.78	4 ± 0	< 0.0001
Motor score	5.37 ± 1.65	8 ± 0	< 0.0001
Sensory deficit	2.87 ± 1.48	6 ± 0	< 0.0001
Sphincter dysfunction	2.57 ± 0.73	3 ± 0	< 0.0001

JOA, Japanese Orthopedic Association.

Region-of-interest analysis

The region-of-interests (ROIs) for the present study were the subdivision structures of S1 (BA1, BA2, and BA3), M1 (BA4a and BA4p), SAC (BA5), and SMA (BA6). All these structures have been reported in previous research to be areas altered in patients with CSM [4–7,9,11]. The WFU PickAtlas toolbox (*http://fmri.wfubmc.edu/software/PickAtlas/*) [21,22] and SPM anatomy toolbox version 2.2b (*http://www.fz-juelich.de/inm/inm-1/EN/Forschung/_docs/SPMAnatomyToolbox*) [23,24] were used to generate multiple ROIs separately for the left and the right hemispheres. The ROIs were then resliced to our own data.

Statistical analysis

A two-sample *t*-test was performed and used with the Data Processing Assistant for Resting-State fMRI Advanced Edition (DPARSFA) v2.3 (*http://www.restfmri.net*) toolbox to compare the CSM patients with the healthy controls [25]. Age and education were modeled as covariates of no interest. The statistical significance of the group differences in each region was set to a *P* value of less than 0.01 at the voxel level, to a *P* value of less than 0.05 at the cluster level, and to a cluster size of greater than or equal to 30. Multiple comparisons were corrected using the AlphaSim method. To determine the correlations between volume and symptoms, a peak point was used as the center of a sphere with a 6-mm radius, which was retrieved from the volume analysis as an area of significant atrophy. These spheres were used as new ROIs to extract the average values for the volume of gray matter in patients with CSM. They were then correlated with the clinical characteristics of the patients, such as the JOA score, upper motor score, lower motor score, sensory score, and sphincter dysfunction score, using Pearson's correlation analysis. SPSS v22.0 was used for the statistical analyses (SPSS Inc., Chicago, Illinois, USA).

Results

Demographic and clinical characteristics

Table 1 shows the demographic and clinical data for the CSM patients and healthy controls. There were no

significant differences in age, sex, or years of education between the CSM patients and health controls (HCs) ($P > 0.05$).

Group differences in gray matter

Table 2 shows group-level differences in gray matter volume between the CSM patients and HCs (AlphSim corrected, voxel level, $P < 0.01$; cluster level and cluster > 30, $P < 0.05$; Fig. 1). The HCs had significantly larger volumes of gray matter in the left BA1 (peak MNI coordinates: $x = -49.5$, $y = -22.5$, $z = 58.5$; cluster size = 50 voxels; peak $t = 3.11$), left BA2 (peak MNI coordinates: $x = -42$, $y = -31.5$, $z = 42$; cluster size = 67 voxels; peak $t = 3.13$), left BA3a (peak MNI coordinates: $x = -40.5$, $y = -22.5$, $z = 33$; cluster size = 40 voxels; peak $t = 3.21$), right BA3a (peak MNI coordinates: $x = 37.5$, $y = 21$, $z = 39$; cluster size = 59 voxels; peak $t = 3.31$), left BA3b (peak MNI coordinates: $x = -42$, $y = -24$, $z = 34.5$; cluster size = 43 voxels; peak $t = 3.12$), left BA4a (peak MNI coordinates: $x = -42$, $y = -24$, $z = 34.5$; cluster size = 218 voxels; peak $t = 4.14$), right BA4p (peak MNI

Fig. 1

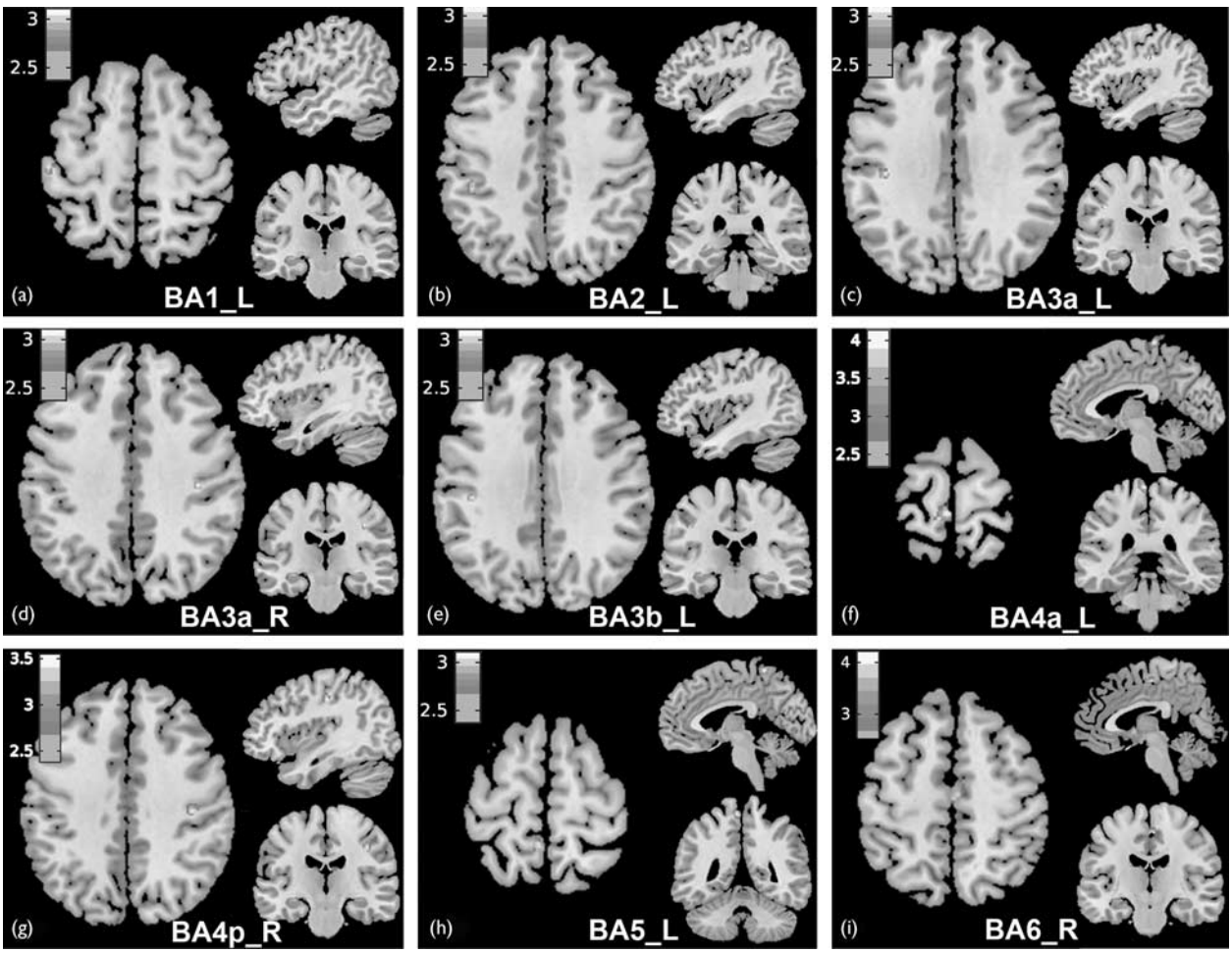

Atrophy volume in sensorimotor cortices. (a) The volumes of BA1_L were significantly larger in the healthy control group than in the CSM patient group (cluster size = 50 voxels, $t = 3.11$, voxel level, $P < 0.01$, cluster level, $P < 0.05$, AlphaSim corrected). (b) The volumes of BA2_L were significantly larger in the healthy control group than in the CSM patient group (cluster size = 67 voxels, $t = 3.13$, voxel level, $P < 0.01$, cluster level, $P < 0.05$, AlphaSim corrected). (c) The volumes of BA3a_L were significantly larger in the healthy control group than in the CSM patient group (cluster size = 40 voxels, $t = 3.21$, voxel level, $P < 0.01$, cluster level, $P < 0.05$, AlphaSim corrected). (d) The volumes of BA3a_R were significantly larger in the healthy control group than in the CSM patient group (cluster size = 59 voxels, $t = 3.31$, voxel level, $P < 0.01$, cluster level, $P < 0.05$, AlphaSim corrected). (e) The volumes of BA3b_L were significantly larger in the healthy control group than in the CSM patient group (cluster size = 43 voxels, $t = 3.12$, voxel level, $P < 0.01$, cluster level, $P < 0.05$, AlphaSim corrected). (f) The volumes of BA4a_L were significantly larger in the healthy control group than in the CSM patient group (cluster size = 218 voxels, $t = 4.13$, voxel level, $P < 0.01$, cluster level, $P < 0.05$, AlphaSim corrected). (g) The volumes of BA4p_R were significantly larger in the healthy control group than in the CSM patient group (cluster size = 78 voxels, $t = 3.55$, voxel level, $P < 0.01$, cluster level, $P < 0.05$, AlphaSim corrected). (h) The volumes of BA5_L were significantly larger in the healthy control group than in the CSM patient group (cluster size = 115 voxels, $t = 3.35$, voxel level, $P < 0.01$, cluster level, $P < 0.05$, AlphaSim corrected). (i) The volumes of BA6_R were significantly larger in the healthy control group than in the CSM patient group (cluster size = 90 voxels, $t = 4.21$, voxel level, $P < 0.01$, cluster level, $P < 0.05$, AlphaSim corrected). BA, Brodmann area; CSM, cervical spondylotic myelopathy.

Fig. 2

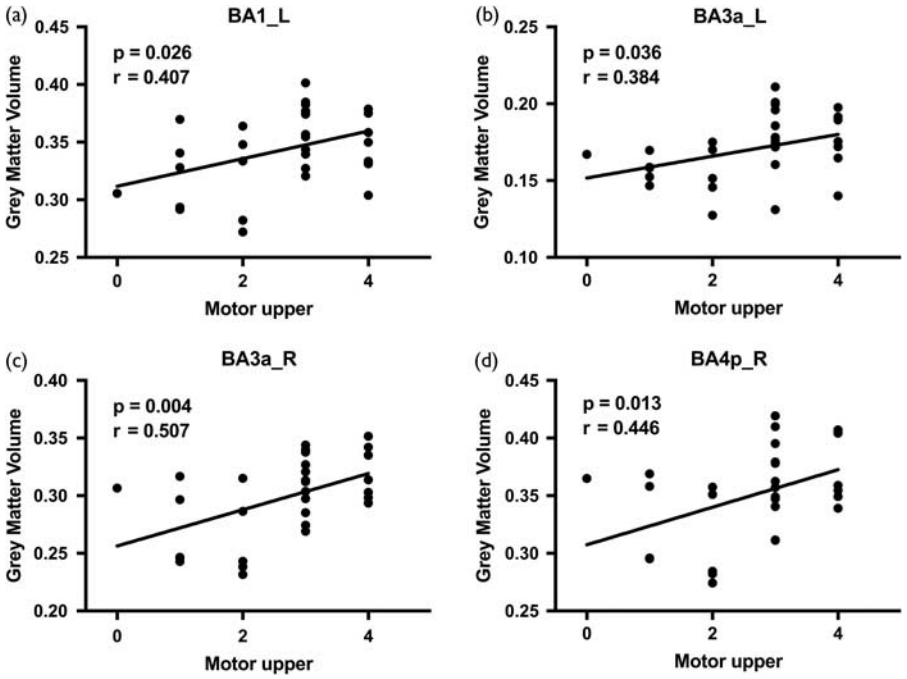

Correlations between the volume of atrophied gray matter and upper motor scores. Scatterplots show the positive correlations between changes in (a) the left BA1 ($r = 0.407$, $P = 0.026$), (b) left BA3a ($r = 0.407$, $P = 0.026$), (c) right BA3a ($r = 0.507$, $P = 0.004$), and (d) right BA4p ($r = 0.446$, $P = 0.013$) and the upper motor scores ($P < 0.05$). BA, Brodmann area.

Fig. 3

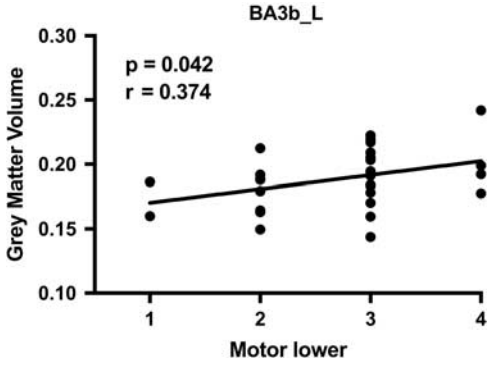

Correlations between the volume of atrophied gray matter and lower motor score. Scatterplots show the correlations between changes in the volume of left BA3b ($r = 0.374$, $P = 0.042$) and the lower motor scores ($P < 0.05$). BA, Brodmann area.

Fig. 4

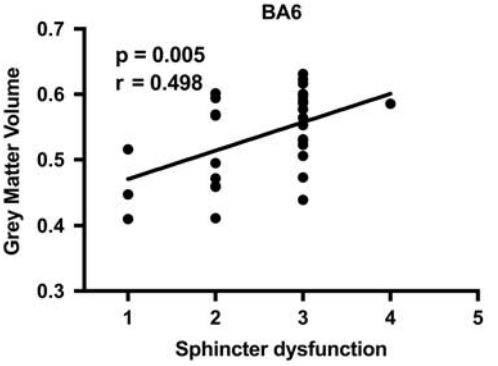

Correlations between the volume of atrophied gray matter and sphincter dysfunction score. Scatterplots show the correlations between changes in the volume of left BA6 ($r = 0.497$, $P = 0.005$) and the sphincter dysfunction scores ($P < 0.05$). BA, Brodmann area.

coordinates: $x = 39$, $y = -19.5$, $z = 40.5$; cluster size = 78 voxels; peak $t = 3.55$), left BA5 (peak MNI coordinates: $x = -4.5$, $y = -46.5$, $z = 64.5$; cluster size = 115 voxels; peak $t = 3.25$), and left BA6 (peak MNI coordinates: $x = 3$, $y = -16.5$, $z = 52.5$; cluster size = 90 voxels; peak $t = 4.22$). There were no significant differences in gray matter volume in the right BA1, right BA2, right BA3b, right BA4a, left BA4p, right BA5, and right BA6.

Correlation of volume with clinical indicators

Table 3 shows the correlations of gray matter volume with the clinical scores ($P < 0.05$). There was a significant correlation between the gray matter volumes in the left BA1, left BA3a, right BA3a, left BA3b, and right BA4p and the motor scores. The gray matter volumes for the left BA1 ($r = 0.407$, $P = 0.026$), left BA3a ($r = 0.407$, $P = 0.026$), right BA3a ($r = 0.507$, $P = 0.004$), and right

BA4p ($r=0.446$, $P=0.013$) were correlated positively with the upper motor scores. The gray matter volume for the left BA3b ($r=0.374$, $P=0.042$; Fig. 2) was correlated positively with the lower motor scores. The gray matter volume for left BA6 ($r=0.497$, $P=0.005$; Fig. 3) was correlated positively with the sphincter dysfunction scores (Fig. 4). The gray matter volume was not correlated significantly in any area with the JOA scores or the sensory scores. No significant correlations were observed between the gray matter volume atrophy and the clinical scale observed in left BA2, left BA4a, and left BA5.

Discussion

Neurological injury can cause neuronal plasticity, which leads to the reorganization of cortical networks in the brain. In the past, synaptic plasticity has been shown in a number of neurological disorders, including multiple sclerosis, stroke, and SCI [26,27]. Several studies have shown that cortical reorganization is present in SCI patients, including both structural and functional reorganization. Previous animal studies have shown significant reductions in the volumes of the sensorimotor cortices [1] and various studies have reported gray matter atrophy in the motor cortices of patients with SCI [3,4].

Table 2 Atrophied area in the sensorimotor cortex

	MNI			Voxel	Peak
	x	*y*	*z*	Size	*t*-value
S1					
BA1_L	−49.5	−22.5	58.5	50	3.1096
BA2_L	−42	−31.5	42	67	3.1278
BA3a_L	−40.5	−22.5	33	40	3.2092
BA3a_R	37.5	−21	39	59	3.3157
BA3b_L	−42	−24	34.5	43	3.121
M1					
BA4a_L	−4.5	−33	73.5	218	4.1376
BA4p_R	39	−19.5	40.5	78	3.5496
SAC					
BA5_L	−4.5	−46.5	64.5	115	3.2465
SMA					
BA6_R	3	−16.5	52.5	90	4.2157

BA, Brodmann area; M1, primary motor cortex; MNI, Montreal Neurological Institute; S1, primary somatosensory cortex; SAC, somatosensory association cortex; SMA, supplementary motor area; SMA, supplementary motor area. AlphSim corrected, voxel level, $P<0.01$; cluster level, $P<0.05$.

CSM is a chronic SCI and provides a unique model of SCI, with similar cervical spinal damage, but potentially reversible neurological changes [16,28]. Previous fMRI studies have reported that CSM patients undergo significant functional reorganization of the sensorimotor system in response to their motor and sensory function deficits [5–7]. Other studies have reported that task-fMRI, which requires participants to perform motions such as wrist extension or finger tapping, identified changes in the activation volume in the sensorimotor cortices of the CSM patients [5–7,11]. A study by Dong *et al.* [6] indicated that CSM patients have smaller activation volumes in M1, S1, and dorsal PMA than healthy controls during dexterous finger tapping. However, different results were reported by another study, which showed an increased activation volume within the precentral gyrus and a reduced activation volume within the postcentral gyrus of the CSM patients compared with the healthy controls [5]. Some studies have reported increased amplitude of the low-frequency fluctuations and increased functional connectivity strength in the sensorimotor cortices of CMS patients on resting-state-fMRI [9,29]. These findings suggest that the activation of the contralateral gray matter increases to compensate for spinal cord compression. However, it is currently unclear whether the sensorimotor cortex enlarges or atrophies in patients with CSM.

In the present study, we found significant atrophy in the left BA1, left BA2, left BA3a, left BA3a, left BA3b, left BA4a, right BA4p, left BA5, and left BA6 in the CSM patients. These findings may contradict previous research indicating that CSM patients showed larger activation volume during motor tasks than HCs [6,7]. However, the increased volume of activation does not mean that the volume of the gray matter is increased. Because CSM is a chronic SCI and has lesions similar to lesions in acute SCI, the sensorimotor cortex in CSM patients is atrophied as found in patients with acute SCI. The present study suggests that the increased activation in the sensorimotor cortices is a compensatory mechanism for the atrophy of the sensorimotor cortices. Unlike acute SCI, CSM is a long-term progressive disease with

Table 3 Correlation of the activation area with clinical information ($P<0.05$)

	Correlation coefficient (*P* value)				
	JOA	Motor upper	Motor lower	Sensory	Sphincter
BA1_L	0.243 (0.195)	0.407 (0.026)	0.29 (0.120)	−0.081 (0.670)	0.188 (0.323)
BA2_L	0.160 (0.399)	0.290 (0.120)	0.192 (0.309)	−0.060 (0.752)	0.101 (0.596)
BA3a_L	0.156 (0.409)	0.384 (0.036)	0.324 (0.081)	−0.148 (0.435)	−0.021 (0.911)
BA3a_R	0.243 (0.195)	0.507 (0.004)	0.189 (0.317)	−0.003 (0.988)	−0.018 (0.926)
BA3b_L	0.109 (0.566)	0.292 (0.117)	0.374 (0.042)	−0.180 (0.341)	−0.057 (0.765)
BA4a_L	0.136 (0.474)	0.306 (0.101)	−0.059 (0.757)	−0.026 (0.890)	0.183 (0.332)
BA4p_R	0.210 (0.266)	0.446 (0.013)	0.195 (0.301)	−0.043 (0.822)	0.188 (0.922)
BA5_L	0.184 (0.331)	0.267 (0.154)	−0.164 (0.387)	0.117 (0.5381)	0.256 (0.173)
BA6_L	0.316 (0.089)	0.341 (0.065)	0.162 (0.393)	−0.222 (0.237)	0.497 (0.005)

BA, Brodmann area; JOA, Japanese Orthopedic Association; L, left; R, right.

incomplete SCI. Hence, there is more time to expand the areas of activation in the sensorimotor cortices, which will compensate for the loss of volume. This theory may shed light on the discrepancies in the previous findings. Several studies have reported an increased volume of activation in multiple cortices, whereas other studies have shown reduced volumes of activation [5–7,11]. In the early stages of CSM, atrophy is present in the sensorimotor cortices, together with reduced activation. However, as compensation progresses, the activation in some parts of the sensorimotor cortices increases. Therefore, the sensorimotor cortices experience different levels of activation at different stages of CSM. It is noteworthy that there may be no evidence of symptoms in the early stages of CSM, which makes it difficult to define each stage.

BA4a and BA4p are separated in the premotor cortex (BA4), corresponding to their distinct cytoarchitectural and receptor density characteristics [15]. However, as somatotopically organized areas are present within both the subregions, both have a specific and an inclusive function [13]. BA4a is considered to be more 'executive', which means that it is responsible for actual movement, whereas BA4p participates in cognitive tasks or non-executive functions. In the present study, the left BA4a and right BA4p showed significant atrophy. Thus, the right BA4p correlated with the upper motor scores. We speculate that the changes in the contralateral BA4a are responsible for the relative limb dysfunction. Therefore, most CSM patients suffer a loss of manual dexterity, difficulty in writing, and abnormal sensations in the right hand because these executive movement dysfunctions are attributable to the atrophy in the left BA4a. Previous research has reported that the involvement of BA4p appears to be related to the integrity of the corticospinal tract and motor recovery after stroke [30,31]. This suggests that the upper dysfunction of CSM patients should recover after surgery because it is dependent on the degree of atrophy in BA4p.

Our results show that atrophy at the left BA3b is correlated with the lower motor scores, and atrophy at the left BA1, left BA3a, and right BA3a is correlated with the upper motor scores. BA1, BA2, and BA3 make up S1 of the human brain, whereas BA5 is the SAC. However, there was no significant correlation of atrophy in these sensory cortices with the sensory scores. Our results suggest that cortical atrophy may cause motor dysfunction, which contradicts the known functions of these cortices. The diverse symptoms of CSM patients can be attributed to these conflicting results.

The volume of gray matter in the right BA6 showed significantly more atrophy in the CSM patients than in the healthy controls, but did not correlate significantly with the motor scores or the sensory scores. This indicates that in BA6, atrophy is a factor in the loss of sphincter control, consistent with the findings of previous studies [32]. On the basis of our results and previous studies, we suggest that the amount of atrophy in BA6 influences the recovery of sphincter function.

Several limitations must be considered when interpreting the results of the present study. First, although all the participants in our study were younger than 65 years of age, the aging effect cannot be eliminated. Therefore, to ensure that age has a minimal effect on the analysis of gray matter atrophy, future long-term studies should include younger patients. Second, the severity of JOA scores was heterogeneous between inpatients with CSM in this study. The atrophy in sensorimotor cortices exemplified asymmetry which is caused by various symptoms. However, the CSM patient group could not be divided into different subgroups because the sample size was too small. Future studies should investigate the pathophysiology of CSM-related neuroanatomical changes in terms of various symptoms. Third, this present study was cross-sectional; thus, it provides no insight into the dynamic changes that occur in the sensorimotor cortices. Ongoing and future follow-up studies are required to document the full time-course of CSM-related cortical atrophy.

Conclusion

To our knowledge, this is the first study to report this type of information on the structural changes that occur in the sensorimotor cortices of CSM patients. Our findings show significant atrophy in the sensorimotor cortices, which may provide new insights into the compensatory mechanisms present in CSM patients. On the basis of previous findings and the findings of the present study, we suggest that chronic spinal cord compression initially causes atrophy of the sensorimotor cortices and then the activation areas in the sensorimotor cortex begin to expand as a compensatory mechanism.

Acknowledgements

The authors thank Qun Li and Fei Qi for their help in collecting the data. The authors greatly appreciate the advice of Bing Yu in the collecting and postprocessing of data. The authors also thank all the CSM patients and the healthy volunteers who graciously took part in this project.

Conflicts of interest

There are no conflicts of interest.

References

1 Kim BG, Dai HN, McAtee M, Vicini S, Bregman BS. Remodeling of synaptic structures in the motor cortex following spinal cord injury. *Exp Neurol* 2006; **198**:401–415.
2 Martinez M, Rossignol S. A dual spinal cord lesion paradigm to study spinal locomotor plasticity in the cat. *Ann N Y Acad Sci* 2013; **1279**:127–134.
3 Freund P, Weiskopf N, Ward NS, Hutton C, Gall A, Ciccarelli O, *et al.* Disability, atrophy and cortical reorganization following spinal cord injury. *Brain* 2011; **134** (**Pt 6**):1610–1622.

4 Hou JM, Yan RB, Xiang ZM, Zhang H, Liu J, Wu YT, *et al*. Brain sensorimotor system atrophy during the early stage of spinal cord injury in humans. *Neuroscience* 2014; **266**:208–215.
5 Duggal N, Rabin D, Bartha R, Barry R, Gati J, Kowalczyk I, *et al*. Brain reorganization in patients with spinal cord compression evaluated using fMRI. *Neurology* 2010; **74**:1048–1054.
6 Dong Y, Holly LT, Albistegui-Dubois R, Yan X, Marehbian J, Newton JM, *et al*. Compensatory cerebral adaptations before and evolving changes after surgical decompression in cervical spondylotic myelopathy. *J Neurosurg Spine* 2008; **9**:538–551.
7 Holly LT, Dong Y, Albistegui-DuBois R, Marehbian J, Dobkin B. Cortical reorganization in patients with cervical spondylotic myelopathy. *J Neurosurg Spine* 2007; **6**:544–551.
8 Tan Y, Zhou F, Wu L, Liu Z, Zeng X, Gong H, *et al*. Alteration of regional homogeneity within the sensorimotor network after spinal cord decompression in cervical spondylotic myelopathy: a resting-state fMRI study. *Biomed Res Int* 2015; **2015**:647958.
9 Zhou F, Gong H, Liu X, Wu L, Luk KD, Hu Y. Increased low-frequency oscillation amplitude of sensorimotor cortex associated with the severity of structural impairment in cervical myelopathy. *PLoS One* 2014; **9**:e104442.
10 Zhou FQ, Tan YM, Wu L, Zhuang Y, He LC, Gong HH. Intrinsic functional plasticity of the sensory-motor network in patients with cervical spondylotic myelopathy. *Sci Rep* 2015; **5**:9975.
11 Bhagavatula ID, Shukla D, Sadashiva N, Saligoudar P, Prasad C, Bhat DI. Functional cortical reorganization in cases of cervical spondylotic myelopathy and changes associated with surgery. *Neurosurg Focus* 2016; **40**:E2.
12 Craig A, Zhang ET. Retrograde analyses of spinothalamic projections in the macaque monkey: input to posterolateral thalamus. *J Comp Neurol* 2006; **499**:953–964.
13 Geyer S, Ledberg A, Schleicher A, Kinomura S, Schormann T, Burgel U, *et al*. Two different areas within the primary motor cortex of man. *Nature* 1996; **382**:805–807.
14 Zilles K, Amunts K. Centenary of Brodmann's map – conception and fate. *Nat Rev Neurosci* 2010; **11**:139–145.
15 Sanes JN, Donoghue JP. Plasticity and primary motor cortex. *Ann Rev Neurosci* 2000; **23**:393–415.
16 Wu JC, Ko CC, Yen YS, Huang WC, Chen YC, Liu L, *et al*. Epidemiology of cervical spondylotic myelopathy and its risk of causing spinal cord injury: a national cohort study. *Neurosurg Focus* 2013; **35**:E10.
17 Ashburner J, Friston KJ. Unified segmentation. *Neuroimage* 2005; **26**:839–851.
18 Ashburner J. A fast diffeomorphic image registration algorithm. *Neuroimage* 2007; **38**:95–113.
19 Ashburner J. Computational anatomy with the SPM software. *Magn Reson Imaging* 2009; **27**:1163–1174.
20 Ashburner J, Friston KJ. Computing average shaped tissue probability templates. *Neuroimage* 2009; **45**:333–341.
21 Lancaster JL, Woldorff MG, Parsons LM, Liotti M, Freitas CS, Rainey L, *et al*. Automated Talairach atlas labels for functional brain mapping. *Hum Brain Mapp* 2000; **10**:120–131.
22 Maldjian JA, Laurienti PJ, Kraft RA, Burdette JH. An automated method for neuroanatomic and cytoarchitectonic atlas-based interrogation of fMRI data sets. *Neuroimage* 2003; **19**:1233–1239.
23 Eickhoff SB, Stephan KE, Mohlberg H, Grefkes C, Fink GR, Amunts K, *et al*. A new SPM toolbox for combining probabilistic cytoarchitectonic maps and functional imaging data. *Neuroimage* 2005; **25**:1325–1335.
24 Eickhoff SB, Paus T, Caspers S, Grosbras MH, Evans AC, Zilles K, *et al*. Assignment of functional activations to probabilistic cytoarchitectonic areas revisited. *Neuroimage* 2007; **36**:511–521.
25 Yan CG, Wang XD, Zuo XN, Zang YF. DPABI: data processing & analysis for (resting-state) brain imaging. *Neuroinformatics* 2016; **14**:339–351.
26 Husted CA, Matson GB, Adams DA, Goodin DS, Weiner MW. In vivo detection of myelin phospholipids in multiple sclerosis with phosphorus magnetic resonance spectroscopic imaging. *Ann Neurol* 1994; **36**:239–241.
27 Puri BK, Smith HC, Cox IJ, Sargentoni J, Savic G, Maskill DW, *et al*. The human motor cortex after incomplete spinal cord injury: an investigation using proton magnetic resonance spectroscopy. *J Neurol Neurosurg Psychiatry* 1998; **65**:748–754.
28 Baron EM, Young WF. Cervical spondylotic myelopathy: a brief review of its pathophysiology, clinical course, and diagnosis. *Neurosurgery* 2007; **60** (**Supp 11**):S35–S41.
29 Zhou F, Wu L, Liu X, Gong H, Luk KD, Hu Y. Characterizing thalamocortical disturbances in cervical spondylotic myelopathy: revealed by functional connectivity under two slow frequency bands. *PLoS One* 2015; **10**: e0125913.
30 Ward NS, Brown MM, Thompson AJ, Frackowiak RS. Neural correlates of motor recovery after stroke: a longitudinal fMRI study. *Brain* 2003; **126** (**Pt 11**):2476–2496.
31 Ward NS, Newton JM, Swayne OB, Lee L, Thompson AJ, Greenwood RJ, *et al*. Motor system activation after subcortical stroke depends on corticospinal system integrity. *Brain* 2006; **129** (**Pt 3**):809–819.
32 Deutsch G, Deshpande H, Frolich MA, Lai HH, Ness TJ. Bladder distension increases blood flow in pain related brain structures in subjects with interstitial cystitis. *J Urol* 2016; **196**:902–910.